J. Eng. Technol. Sci., Vol. 53, No. 3, 2021, 210306

Airflow Characteristics Investigation of a Diesel Engine for Different Helical Port Openings and Engine Speeds

Willyanto Anggono[1,2], Mitsuhisa Ichiyanagi[3], Reina Saito[3], Gabriel J. Gotama[2], Chris Cornelius[1,2], Ryera Kreshna[1,2] & Takashi Suzuki[3]

[1]Mechanical Engineering Department, Petra Christian University, Jalan Siwalankerto No. 121-131, Wonocolo, Surabaya, Jawa Timur 60236, Indonesia
[2]Centre for Sustainable Energy Studies, Petra Christian University, Jalan Siwalankerto No. 121-131, Wonocolo, Surabaya, Jawa Timur 60236, Indonesia
[3]Department of Engineering and Applied Sciences, Sophia University, 7-1 Kioi-cho, Chiyoda-ku, Tokyo 102-8554, Japan
*E-mail: willy@petra.ac.id

Highlights:

- Variation of engine speed and helical port opening did not cause significant changes in the location of the swirl center.
- A higher engine speed increased the turbulence intensity but reduced the swirl ratio.
- Disruption of the airflow with a larger helical port opening reduced both the swirl ratio and the turbulence intensity.
- The trends of swirl ratio and turbulence intensity were more evident when observed during the compression stroke.

Abstract. Intake airflow characteristics are essential for the performance of diesel engines. However, previous investigations of these airflow characteristics were mostly performed on two-valve engines despite the difference between the airflow of two-valve and four-valve engines. Therefore, in this study, particle image velocimetry (PIV) investigations were performed on a four-valve diesel engine. The investigations were conducted under different engine speeds and helical port openings using a swirl control valve (SCV). The results suggest that the position of the swirl center does not significantly shift with different engine speeds and helical port openings, as the dynamics of the flow remained closely similar. The trends of the airflow characteristics can be best observed during the compression stroke. A higher engine speed increases the angular velocity of the engine more compared to the increase of the airflow velocity and results in a lower swirl ratio of the flow. On the other hand, a higher engine speed leads to a higher mean velocity and the variation of velocity results in a larger turbulence intensity of the flow. Increasing the helical port opening brings a reduction in the swirl ratio and turbulence intensity as more airflow from the helical port disturbs the airflow from the tangential port.

Keywords: *airflow; particle image velocimetry; swirl control valve; swirl ratio; turbulence intensity*.

Received August 12th, 2020, Revised October 21st, 2020, Accepted for publication 19 November 2020.
 ISSN: 2337-5779,
DOI: 10.5614/j.eng.technol.sci.2021.53.3.6

1 Introduction

Diesel engines are the most used engines in commercial land-based vehicles due to their higher thermal efficiency in comparison with gasoline engines [1]. Over recent years, the increased energy demand due to the rise in the global population [2], overreliance on fossil fuels [3], and the need to decrease emissions [4-6] have led to more stringent regulations on the design of engines. Several methods have been devised to improve the emissions of diesel engines, including the use of biofuel [7,8], manipulating the air mass intake and temperature [9] as well as generating swirl and tumble motion in the airflow.

In a diesel engine, swirl flow may be generated using a helical intake port; this is considered to be more essential than the tumble motion [10]. Swirl flow promotes turbulence characteristics in the airflow for better mixing of the fuel-air mixture through the disintegration of the molecules in the fuel [11,12]. Swirl flow reduces the ignition delay in the combustion process, which leads to reduced soot and NOx emissions [13,14], even though reducing simultaneous soot and NOx emissions is usually considered difficult to achieve, as there is a trade-off between them [1]. Swirl flow has also been found to reduce the burning duration, increase the flame speed, extend the flammability limit, increase the thermodynamic heat transfer, and improve the thermal efficiency in the combustion process [15,16].

Several studies have been performed to understand the parameters that affect the swirl and turbulence characteristics of the airflow in the combustion chamber. Dawat & Venkitachalam [17] conducted a numerical investigation of swirl flow generated by various geometries and orientations of the helical port in a four-valve engine. They suggested that the design and orientation of the helical port affect the swirl ratio and the turbulent kinetic energy. They also found that under similar helical intake port designs, a higher engine speed decreased the swirl ratio and a larger variation of swirl ratio was found at higher engine speed. Catania & Spessa [18] conducted a study using a helicoidal intake port to generate a counterclockwise swirl flow in a two-valve high-squish engine under various engine speeds of 600 to 3000 RPM. They concluded that, for a two-valve engine, an intense high-frequency turbulence production occurs at the intake stroke, which starts to decay at the end of the intake stroke/start of the compression stroke. They also suggest that a trend of mean velocity, turbulence intensity, and mean-velocity fluctuation that scales with the engine speed occurs during most of the compression stage.

Other than the engine speed, the swirl control valve (SCV) also plays a role in the quality of the intake airflow. Kim, *et al.* [19] investigated the effect of the SCV in a tangential port on the flow characteristics at a distance of 37 mm away from the engine head of a four-valve diesel engine. They found an increase in the swirl

ratio by applying SCV closure in the tangential port. However, they also found that the mass flow rate decreased with SCV closure due to the reduced area of the intake port. Matsushita, *et al.* [20] applied an SCV in a helical port of an SI engine and found an increase in the combustion performance due to the high swirl ratio with a closed SCV at partial load. Under full load condition, the SCV allows the engine to consistently have high performance.

While the generation of swirl and turbulence flow in combustion cylinders has been studied extensively, the effect of swirl flow generated by a helical intake port in four-valve diesel engines has not received much attention [17]. Kim, *et al.* [19] have suggested that the airflow characteristics between two-valve and four-valve engines are exceptionally contrasting, indicating the necessity to separately investigate the airflow of a four-valve engine. Furthermore, the effect of various SCV openings on a helical intake port paired with a fully opened tangential intake port also has not been comprehensively investigated. Therefore, in this study, the swirl ratio and the turbulence intensity in the combustion chamber of a four-valve diesel engine were investigated using the particle image velocimetry (PIV) technique under various engine speeds and openings of a helical intake port.

2 Methods

The experiment was conducted using an optical four-stroke single-cylinder diesel engine with four valves. The bore and length stroke of the engine were 85 mm and 96.9 mm, respectively. The cavity diameter of the chamber was 51.6 mm and the engine had a compression ratio of 16.3. One helical and one tangential intake port were used as this combination generates a higher swirl ratio compared to two tangential or two helical ports [21]. The location of the ports as seen from the top of the cylinder and the coordinate axes in the *x*, *y* and *z* directions are shown in Figure 1. A Nd:YAG double-pulse 532-nm laser (Continuum, Mesa-PIV) with pulse generator (Flowtech Research, VSD2000) was used to generate a laser sheet. The laser sheet had a thickness of 1 mm and was irradiated perpendicularly to the center axis of the cylinder and positioned at 60 mm from the top of the cylinder to develop a two-dimensional plane (z = 60 mm). Particle images from the reflection of the mirror were taken from the bottom of the engine with a high-speed camera (Photron, Fastcam SA5) at a resolution of 696 x 704 pixels and a time resolution of 15 kHz. A pair of images per two crank angles (CAD) were taken at an interval of 20 μs. Tracer silica particles (SiO_2) with an average particle size of 4.65 μm were mixed into the intake air using a seeding generator (PivTech GmbH) and an air compressor (Earth Man, ACP-25SLA).

The particle images were analyzed using the PIV (Flowtech Research FtrPIV) analysis software with the direct cross-correlation algorithm [22]. The inspection area was set to 16 pixels and the search area was set to 33 pixels. This setup has

been used by the author in a previous study [23] and another research group has used a similar setup to investigate the airflow characteristics in a combustion cylinder [24]. A photograph and a schematic of the experimental setup are provided in Figure 2.

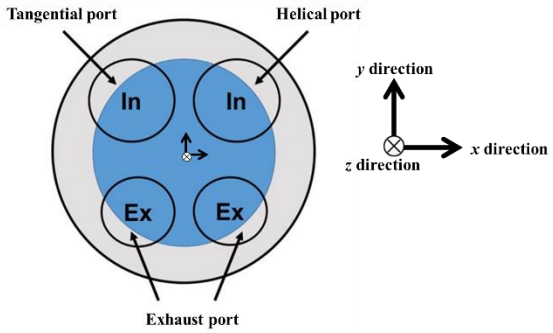

Figure 1 Port location as seen from the top of the combustion cylinder.

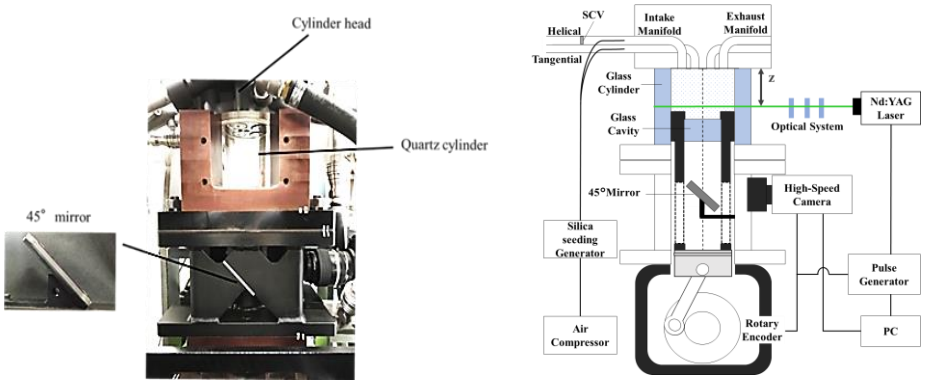

(a) (b)

Figure 2 (a) Photograph of the experimental setup and (b) schematic of the experimental setup.

In this study, two sets of experiments were performed. The first set of experiments was conducted under various engine speeds with fully opened tangential and helical ports, corresponding to a 100% SCV opening. The second set of experiments was conducted under constant engine speed with various openings of the helical port to modify the SCV opening. This is in contrast with the study by Kim, *et al.* [19], where the SCV was applied in the tangential port. For this study, the percentage of SCV opening was defined by the velocity of the flow that passed through the ports. Summaries of the experimental conditions for the first and second set of experiments are given in Tables 1 and 2, respectively.

Table 1 Parameters for the first set of experiments.

Tangential Port Opening	Helical Port Opening	SCV Opening	Engine Speed
100%	100%	100%	1000 RPM
100%	100%	100%	1200 RPM
100%	100%	100%	1500 RPM

Table 2 Parameters for the second set of experiments.

Tangential Port Opening	Helical Port Opening	SCV Opening	Engine Speed
100%	25% (1/4 Helical)	25%	1000 RPM
100%	50% (1/2 Helical)	50%	1000 RPM
100%	75% (3/4 Helical)	75%	1000 RPM
100%	100%	100%	1000 RPM

For both sets of experiments, the engine was operated under naturally aspirated condition. The Stokes number was set to 0.00354, 0.00425, 0.00531, for an engine speed of 1000 RPM, 1200 RPM, 1500 RPM, respectively. The number of cycles measured was 32 consecutive cycles for all conditions, with 0 CAD defined as the TDC of the intake stroke. The experiment was performed in two replications and the average of the results was taken as the mean velocity. The measured mean velocity was used to calculate the swirl ratio and the turbulence intensity. The swirl ratio is defined as the normalized average angular velocity of the rotating flow in the measured plane, as mathematically described in Eq. (1). The turbulence intensity is defined as the resultant of the standard deviation of the velocity, as mathematically described in Eq. (2). More emphasis was put on the results for crank angles of 110, 180, and 250 CAD, which correspond to the condition during the intake stroke, the end of the intake stroke/start of the compression stroke, and during the compression stroke, respectively.

$$S_R = \frac{1}{\omega_{engine}} \frac{1}{N} \sum_{l=1}^{N} \left[\frac{v_{i,j} \cos\theta - u_{i,j} \sin\theta}{r_{i,j}} \right]_l \tag{1}$$

where S_R is the swirl ratio, ω_{engine} is the angular velocity of the engine, N is the total number of discretized points of the plane, θ and $r_{i,j}$ are the angle and Cartesian coordinates of a point, respectively, while $u_{i,j}$ and $v_{i,j}$ are the velocity in the horizontal and vertical directions, respectively.

$$T_I = \frac{1}{N} \sum_{l=1}^{N} \sqrt{\left[(U_{RMS})^2 + (V_{RMS})^2 \right]_l} \tag{2}$$

where T_I is the turbulence intensity, U_{RMS} is the root-mean-square of the velocity in the x direction, and V_{RMS} is the root-mean-square of the velocity in the y-direction.

3 Results and Discussion

3.1 Swirl Ratio and Turbulence Intensity under Various Engine Speeds (First Set of Experiments)

Figure 3 shows the mean velocity profile for various engine speeds at different crank angles. In this figure, the swirl center can be identified as the epicenter of the vectors and has a very low mean velocity.

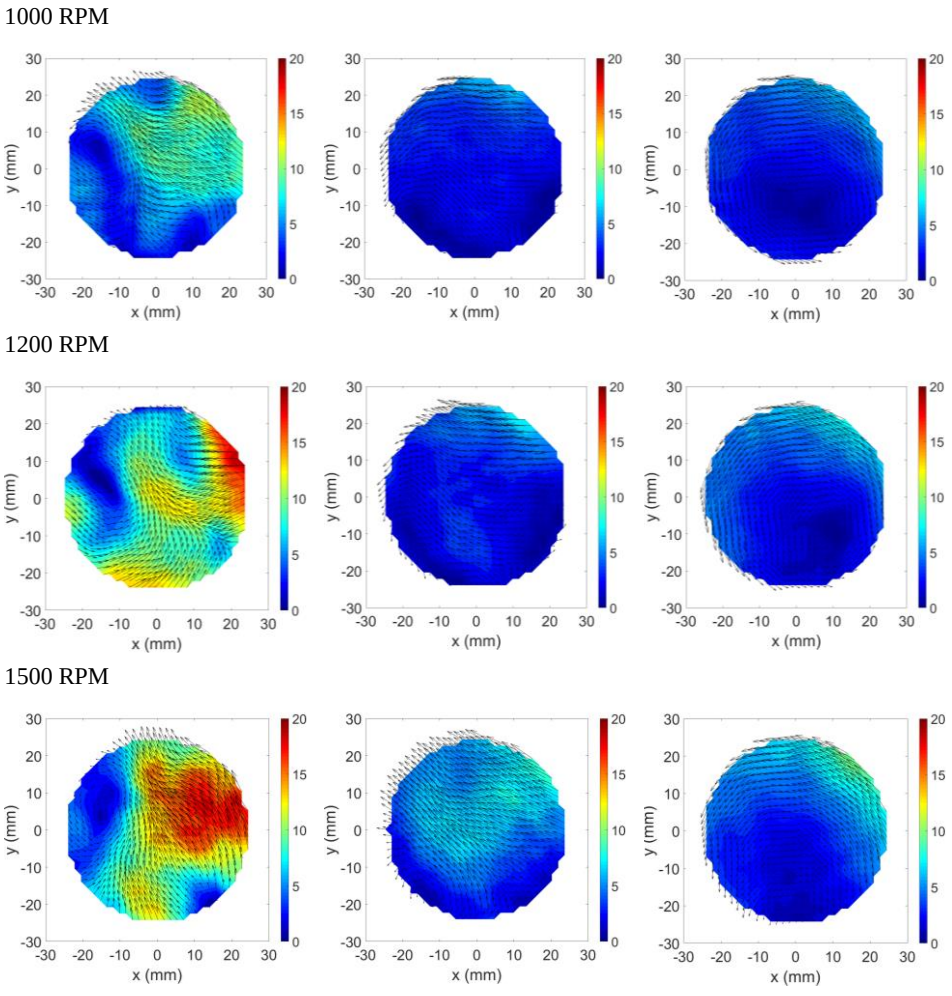

Figure 3 Mean velocity profile (in m/s) of the airflow under various engine speeds at 110, 180, and 250 CAD.

At 110 CAD, the swirl center resided near the tangential port (upper left) for all engine speeds investigated. At 180 CAD, the swirl center was located near the left exhaust port (lower left) for all engine speeds investigated. At 250 CAD, the swirl center was located in the vicinity of the right exhaust port (bottom right) for all engine speeds investigated. These results suggest that an increase in engine speed does not cause a dramatic change of the swirl center. This is because the higher engine speed leads to a similarly larger proportion of the mass flow and mean velocity of the flow for both intake ports, and therefore does not significantly alter the dynamic of the flow within the chamber.

Figure 4 shows the turbulence intensity profile of the cylinder under various engine speeds and crank angles. Unlike the swirl center, it is difficult to pinpoint the maximum turbulence intensity from the figures; therefore, the coordinates for the largest turbulence intensity under various engine speeds and crank angles are given in Table 3.

The overall trend is that the turbulence intensity reduces with lower engine speed and higher crank angle. The location for the maximum turbulence intensity varies between engine speed and crank angle with no clear trend. However, it was observed that for all conditions except 1000 RPM and 250 CAD, the location of the highest turbulence intensity tended to be on the right side near the helical or right exhaust ports. This was expected, as the helical port generates swirl flow in its vicinity, which leads to a large variation in velocity and therefore large turbulence intensity.

To further analyze the results, the swirl ratio and the turbulence intensity were plotted for the entirety of the crank angle. Figure 5(a) shows the swirl ratio as a function of the crank angle for various engine speeds. Near 110 CAD (during the intake stroke), the swirl ratio reached its peak, after which it dramatically decreased with the increase of the crank angle to near 180 CAD (end of intake stroke/start of compression stroke). Near 180 CAD, the swirl ratio started to increase up to 250 CAD (during the compression stroke).

An exception was found at 1000 RPM, where a dip of the swirl ratio occurred earlier (~140 CAD) and therefore the increase of the swirl ratio also started earlier (~150 CAD). A clear trend of the swirl ratio could be observed at compression stroke (180 to 250 CAD) with the swirl ratio tending to be inversely proportional to the engine speed. The reason behind this can be traced in the mathematical definition of swirl ratio in Eq. (1). When the velocity of the flow, which is proportional to the swirl ratio, increases with engine speed, the angular velocity of the engine, which is inversely proportional to the swirl ratio, also increases. However, when the velocity of the flow increases, the airflow interferes with the cylinder and the friction increases. From the above, the increase of the flow

velocity is lower than the increase of the angular velocity of the engine and therefore a higher engine speed reduces the swirl ratio.

Figure 5(b) shows turbulence intensity as a function of crank angle under various engine speeds. There is a clear trend of the turbulence intensity throughout all of the observed crank angles. The flow tends to be highly turbulent during the intake stroke and decreases as it moves towards the compression stroke. The result also suggests that the turbulence intensity is proportional to the engine speed, as a higher engine speed leads to a higher mean velocity, which instigates variation of the velocity and the turbulence behavior of the airflow.

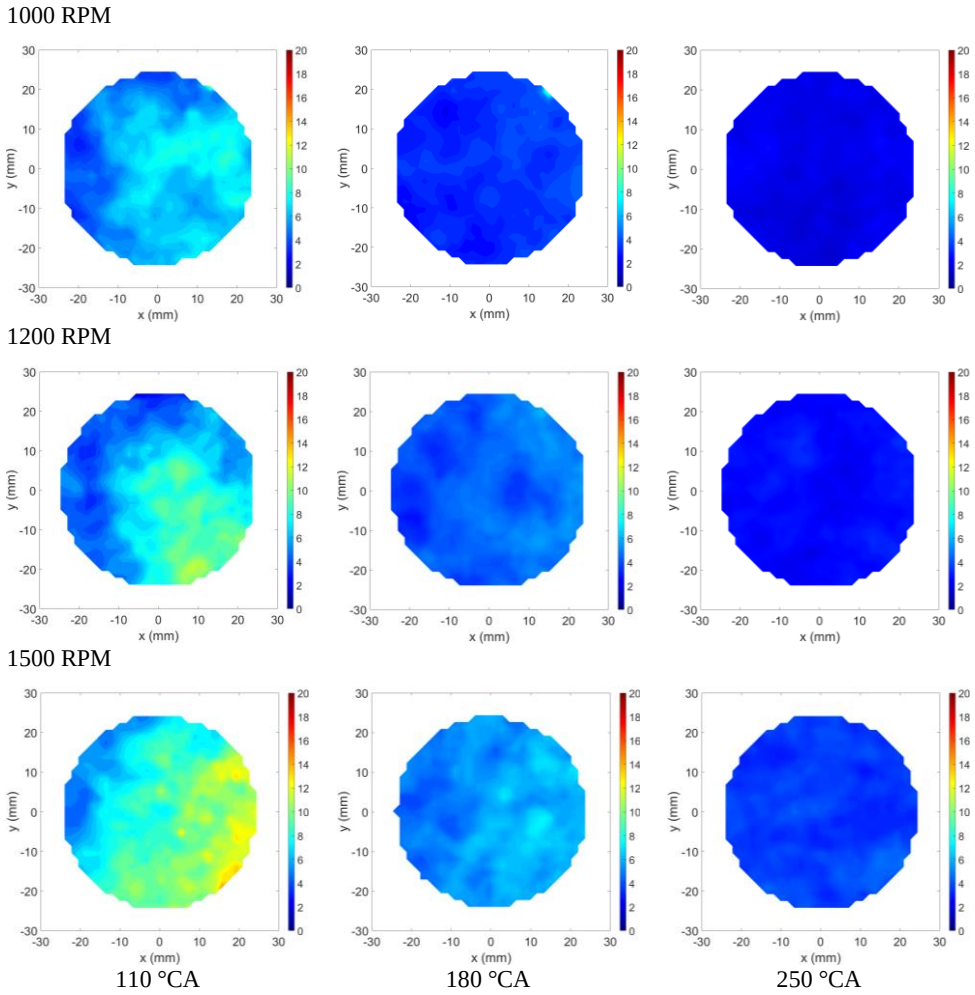

Figure 4 Turbulence intensity profile (in m/s) of the airflow under various engine speeds at 110, 180, and 250 CAD.

Table 3 Coordinates of the maximum turbulence intensity (in mm) under various engine speeds at 110, 180, and 250 CAD.

Parameters	110 CAD	180 CAD	250 CAD
1000 RPM	x = 13.2	x = 14.9	x = -23.4
	y = 21.0	y = 19.3	y = 1.8
1200 RPM	x = 9.9	x = 13.3	x = 20.2
	y = -18.7	y = 19.3	y = 12.4
1500 RPM	x = 15.8	x = 13.3	x = 21.0
	y = -19.0	y = -1.5	y = -12.1

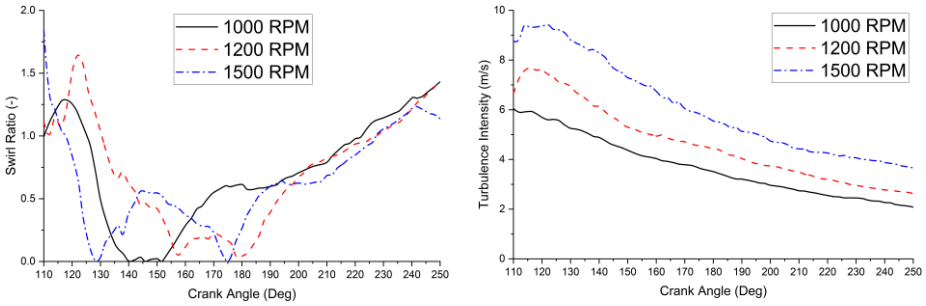

(a) (b)

Figure 5 (a) Swirl ratio and (b) turbulence intensity of the airflow as a function of crank angle under various engine speeds.

3.2 Swirl Ratio and Turbulence Intensity Under Various SCV Openings (Second Set of Experiments)

Figure 6 shows the mean velocity for various helical port openings (percentage of SCV) and crank angles. At 110 CAD, the swirl center was located near the tangential intake port (upper left) and variation of the SCV opening did not cause a significant shift in the location of the swirl center. Similarly, at 180 and 250 CAD, the SCV opening did not change the location of the swirl center, which was located in the vicinity of the left exhaust port (lower left) and the right exhaust port (lower right), respectively. While a smaller SCV opening reduced the intake flow area of the helical port, it merely led to a lower mass flow rate and higher mean velocity of the flow without significantly altering the dynamics of the flow inside the chamber.

As for the turbulence intensity, Figure 7 shows the distribution of turbulence intensity for various helical port openings (SCV openings) and crank angles and Table 4 shows the coordinates for the maximum turbulence intensity.

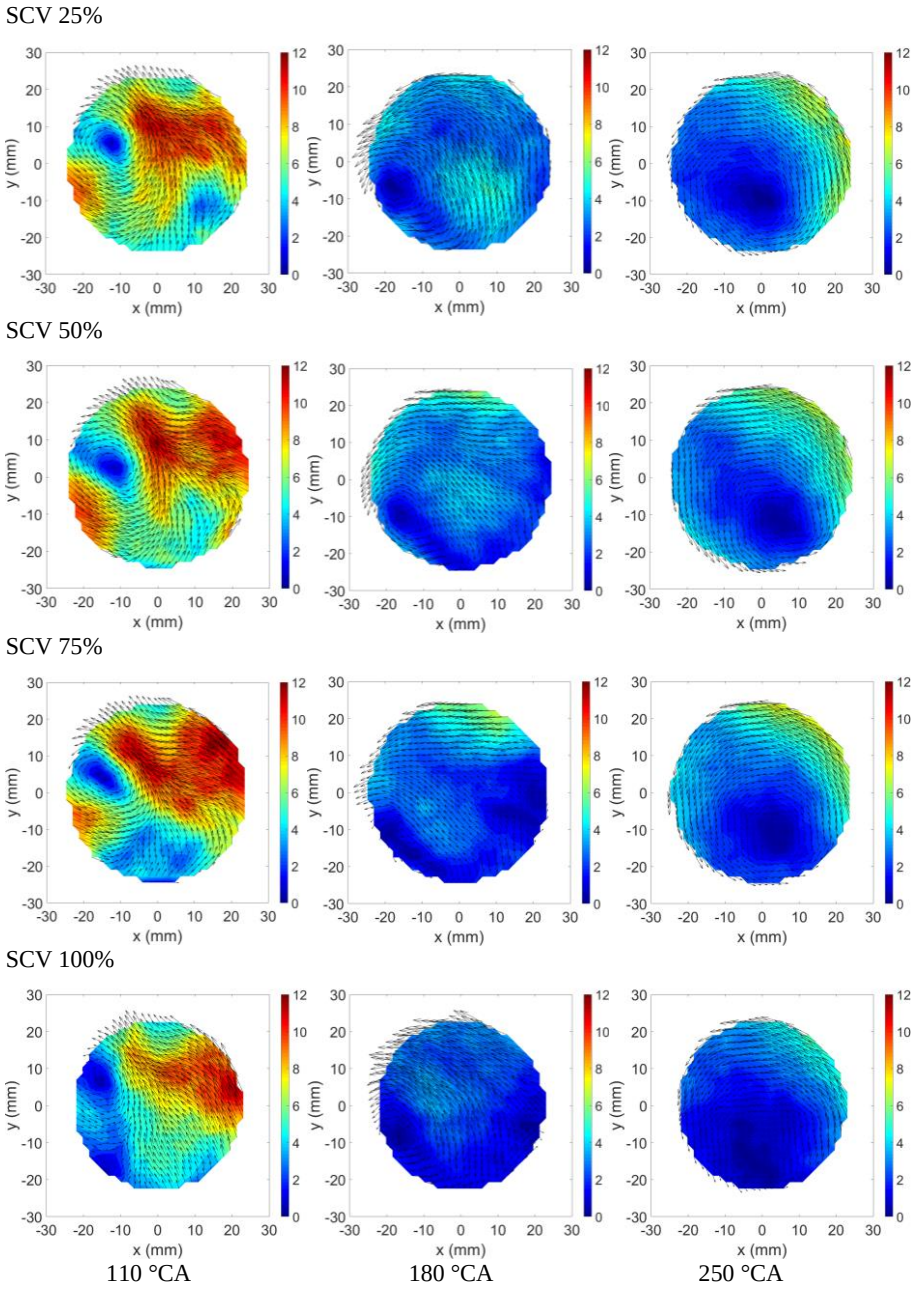

Figure 6 Mean velocity profile (in m/s) of the airflow under various SCV openings at 110, 180, and 250 CAD.

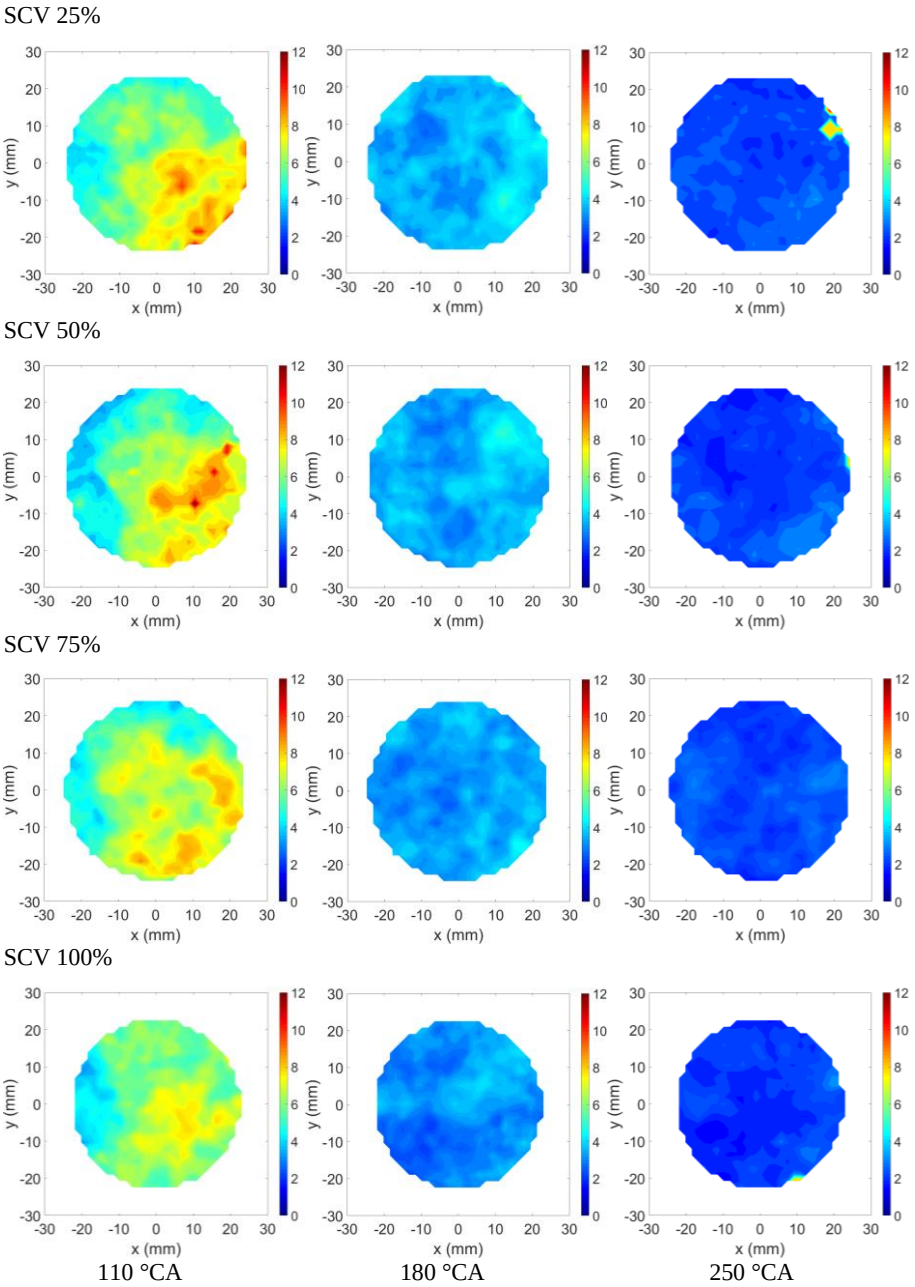

Figure 7 Turbulence intensity profile (in m/s) of the airflow under various SCV openings at 110, 180, and 250 CAD.

It can be inferred that there was a clear trend of a lower turbulence intensity with a larger crank angle. However, in terms of the location of the maximum turbulence intensity, the effect of the SCV opening did not have a clear trend. Similar to the first set of experiments, the majority of the maximum turbulence intensity was located on the right side, either near the helical port or the right exhaust port due to the swirl flow generated by the helical port.

Table 4 Coordinates of the maximum turbulence intensity (in mm) under various SCV openings at 110, 180, and 250 CAD.

Parameters	110 CAD	180 CAD	250 CAD
SCV 25%	x = 10.3	x = 17.2	x = 18.9
	y = -21.9	y = 17.9	y = 14.4
SCV 50%	x = 10.6	x = 10.6	x = 24.4
	y = -7.3	y = 11.7	y = 4.8
SCV 75%	x = -4.0	x = 18.4	x = 15.0
	y = -19.3	y = -15.8	y = 1.5
SCV 100%	x = 7.5	x = 17.8	x = 9.2
	y = -5.1	y = 13.9	y = -20.7

By observing the swirl ratio for all crank angles studied, as shown in Figure 8(a), it was found that the swirl ratio was at its peak during the intake stroke and gradually decreased with a higher crank angle up to a certain angle. Near the start of the compression stroke (~160 to 180 CAD), the swirl ratio increased until 250 CAD. Similar to the first set of experiments, the trend of swirl ratio to crank angle for different SCV openings was observed during the compression stroke. The swirl ratio decreased with larger SCV opening as more mass flow originated from the helical port disrupted the airflow coming from the tangential port, reducing the velocity of the flow inside the chamber.

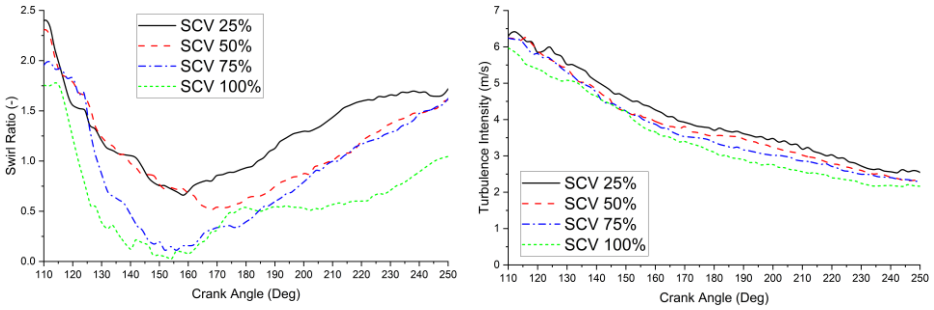

(a) (b)

Figure 8 (a) Swirl ratio and (b) turbulence intensity of the airflow as a function of crank angles under various SCV openings.

Figure 8(b) shows the turbulence intensity of the airflow for all crank angles studied. The turbulence intensity shows a clear trend of a larger SCV opening leading to a lower turbulence intensity. This is due to the larger helical port opening, which disrupts the airflow from the tangential port and reduces the variation of the velocity and turbulence behavior in the airflow of the chamber.

4 Conclusion

The airflow characteristics of a four-valve single-cylinder engine were investigated using the PIV technique for various engine speeds and SCV (helical intake port) openings. The results suggest that the engine speed and SCV opening do not have a significant influence on the location of the swirl center, as the dynamics of the flow inside the chamber remained closely similar. However, a higher engine speed led to a lower swirl ratio, as the angular velocity of the engine increased more in comparison with the velocity of the flow due to the friction between the flow and cylinder. On the other hand, higher engine speed led to higher turbulence intensity due to the increased mean velocity and the variation of the velocity in the flow. As for SCV opening, a higher SCV opening led to a reduction of both the swirl ratio and the turbulence intensity due to the increased mass flow from the helical intake port. This disrupts the airflow coming from the tangential port and reduces the mean velocity as well as the variation of the velocity in the flow. The trends that were found in the present study may be observed more easily during the compression stroke.

Acknowledgments

This research was supported by the Japan Society for the Promotion of Science, Grants-in-Aid for Scientific Research (No. 19K04244), Sophia University Special Grant for Academic Research, Research in Priority Areas, and Petra Christian University under project code: 451/FTI/UKP/2019. The authors would like to express their gratitude towards both Sophia University, Japan, and Petra Christian University, Indonesia, for their support of this study.

Nomenclature

N	=	total number of discretized points [-]
$r_{i,j}$	=	Cartesian coordinates of a point [m]
S_R	=	swirl ratio [-]
T_I	=	turbulence intensity [m/s]
θ	=	angle of a discretized point [rad]
U_{RMS}	=	root mean square of the velocity in the *x*-direction [m/s]
$u_{i,j}$	=	velocity in the horizontal direction [m/s]
V_{RMS}	=	root mean square of the velocity in the *y*-direction [m/s]

$v_{i,j}$ = velocity in the vertical direction [m/s]
ω_{engine} = angular velocity of the engine [rad/s]

References

[1] Anggono, W., Ikoma, W., Chen, H., Liu, Z., Ichiyanagi, M., Suzuki, T. & Gotama, G.J., *Investigation of Intake Pressure and Fuel Injection Timing Effect on Performance Characteristics of Diesel Engine*, IOP Conference Series: Earth and Environmental Science, **257**(1), 012037, May 2019.

[2] Jazie, A.A., *DBSA-catalyzed Sewage Sludge Conversion into Biodiesel in a CSTR: RSM Optimization and RTD Study*, Journal of Engineering and Technological Sciences, **51**(4), pp. 537-555, Aug. 2019.

[3] Mahidin, Gani, A., Muslim, A., Husin, H., Hani, M.R., Syukur, M., Hamdani, K. & Rizal, S., *Sulfur Removal in Bio-Briquette Combustion Using Seashell Waste Adsorbent at Low Temperature*, Journal of Engineering and Technological Sciences, **48**(4), pp. 465-481, Sept. 2016.

[4] Dewi, K., Khair, H. & Irsyad, M., *Development of Green Pavement for Reducing Oxides of Nitrogen (NOx) in the Ambient Air*, Journal of Engineering and Technological Sciences, **48**(2), pp. 159-172, May 2016.

[5] Kodancha, P., Pai, A., Kini, C.R. & Bayar, R.K., *Performance Evaluation of Homogeneous Charge Compression Ignition Combustion Engine-A Review*, Journal of Engineering and Technological Sciences, **52**(3), pp. 289-309, May 2020.

[6] Thonglek, V. & Kiatsiriroat, T., *Use of Pulse-Energized Electrostatic Precipitator to Remove Submicron Particulate Matter in Exhaust Gas*, Journal of Engineering and Technological Sciences, **46**(3), pp. 271-285, Apr. 2014.

[7] Anggono, W., Noor, M.M., Suprianto, F.D., Lesmana, L.A., Gotama, G.J. & Setiyawan, A., *Effect of Cerbera Manghas Biodiesel on Diesel Engine Performance*, International Journal of Automotive and Mechanical Engineering, **15**(3), pp. 5667-5682, Sept. 2018.

[8] Anggono, W., Hayakawa, A., Okafor, E.C., Gotama, G.J. & Wongso, S., *Laminar Burning Velocity and Markstein Length of CH_4/CO_2/Air Premixed Flames at Various Equivalence Ratios and CO_2 Concentrations Under Elevated Pressure*, Combustion Science and Technology, in-press, Mar. 2020. DOI: 10.1080/00102202.2020.1737032.

[9] Yilmaz, E., Ichiyanagi, M. & Suzuki, T., *Development of Heat Transfer Model at Intake System of IC Engine with Consideration of Backflow Gas Effect*, International Journal of Automotive Technology, **20**(5), pp. 1065-1071, Oct. 2019.

[10] Zha, K., Busch, S., Miles, P.C., Wijeyakulasuriya, S., Mitra, S. & Senecal, P.K., *Characterization of Flow Asymmetry During the Compression Stroke Using Swirl-plane PIV in a Light-duty Optical Diesel Engine with the Re-entrant Piston Bowl Geometry*, SAE International Journal of Engines, **8**(4), 2015-01-1699, Apr. 2015.

[11] Agarwal, A.K., Gadekar, S. & Singh, A.P., *In-cylinder Air-flow Characteristics of Different Intake Port Geometries Using Tomographic PIV*, Physics of Fluids, **29**(9), 095104, Sep. 2017

[12] Perini, F., Miles, P.C. & Reitz, R.D., *A Comprehensive Modeling Study of In-cylinder Fluid Flows in a High-swirl, Light-duty Optical Diesel Engine*, Computers and Fluids, **105**, pp. 113-124, Sep. 2014.

[13] Lakshminarayanan, P.A. & Kumar, A., *Design and Development of Heavy-Duty Diesel Engines*, ed. 1, Springer. 2020.

[14] Raj, R.T.K. & Manimaran, R., *Effect of Swirl in a Constant Speed DI Diesel Engine Using Computational Fluid Dynamics*, CFD Letters, **4**(4), pp. 214-224, Dec. 2012.

[15] Hill, P.G. & Zhang, D., *The Effects of Swirl and Tumble on Combustion in Spark-ignition Engines*, Progress in Energy and Combustion Science, **20**(5), pp. 373-429, June 1994.

[16] Varun, Singh, P., Tiwari, S.K., Singh, R. & Kumar, N., *Modification in Combustion Chamber Geometry of CI engines for Suitability of Biodiesel: A review*, Renewable and Sustainable Energy Reviews, **79**, pp. 1016-1033, May 2017.

[17] Dawat, V.K. & Venkitachalam, G., *Influence of a High-Swirling Helical Port with Axisymmetric Piston Bowls on In-Cylinder Flow in a Small Diesel Engine*, SAE Technical Papers, **2016-01-0587**, Apr. 2016.

[18] Catania, A.E. & Spessa, E., *Speed Dependence of Turbulence Properties in a High-squish Automotive Engine Combustion System*, SAE Technical Paper, **105**, pp. 313-334, 1996.

[19] Kim, Y., Han, Y. & Lee, K.A., *Study on the Effects of the Intake Port Configurations on the Swirl Flow Generated in a Small D.I. Diesel Engine*, Journal of Thermal Science, **23**(3), pp. 297-306, May 2014.

[20] Matsushita, S., Inoue, T., Nakanishi, K., Okumura, T. & Isogai, K., *Effects of Helical Port with Swirl Control Valve on the Combustion and Performance of S.I. Engine*, SAE Technical Papers, **94**(850046), pp. 17-22, Feb. 1985.

[21] Jia, D.W., Deng, X.W. & Lei, J.L., *Steady-State Experiment and Simulation of Intake Ports in a Four-valve Direct Injection Diesel Engine*, Journal of Applied Fluid Mechanics, **11**(1), pp. 217-224, 2018.

[22] Raffel, M., Willert, C.E., Wereley, S.T. & Kompenhans, J., *Particle Image Velocimetry*, ed. 1, Springer-Verlag, 2007.

[23] Ichiyanagi, M., Ndizeye, G., Sawamura, Y., Saito, R., Takahashi, K., Otsubo, K., Chen, H. & Takashi, S., *Improvement of on-Board in-Cylinder*

Gas Flow Model and Wall Heat Transfer Prediction Model for CI Engines Using CFD Analysis and PIV Measurements under Motoring and Firing Conditions, SAE Technical Paper, **2019-32-0542**, Jan. 2020.

[24] Petersen, B. & Miles, P., *PIV Measurements in the Swirl-plane of a Motored Light-duty Diesel Engine*, SAE International Journal of Engines, **4**(1), pp. 1623-1641, Apr. 2011.